

TOPOLOGICAL VS GLOBAL PENALTY FORMULATIONS FOR REAL-TIME FLEXIBLE MULTIBODY DYNAMICS

Javier Cuadrado

Escuela Politecnica Superior
University of La Coruña
Ferrol, 15403 SPAIN
Email: javicua@cdf.udc.es

Urbano Lugris

Escuela Politecnica Superior
University of La Coruña
Ferrol, 15403 SPAIN
Email: ulugris@udc.es

Daniel Dopico

Escuela Politecnica Superior
University of La Coruña
Ferrol, 15403 SPAIN
Email: ddopico@udc.es

Manuel Gonzalez

Escuela Politecnica Superior
University of La Coruña
Ferrol, 15403 SPAIN
Email: lolo@cdf.udc.es

ABSTRACT

The simulation of flexible multibody systems is a very demanding task that needs improvements in efficiency in order to achieve real-time performance. One of such improvements may be the use of topological formulations, which have provided good results in the simulation of large rigid multibody systems. In this work, a topological formulation for rigid bodies is extended to the flexible case, and tests are carried out in order to compare its performance with that of a global formulation. Two systems are simulated, a double four-bar mechanism and a vehicle suspension. As it happened in the rigid case for these two examples, the topological formulation shows lower performance than its global counterpart for such small systems, but the difference decreases as more bodies are modeled as flexible. Since in the rigid case the topological formulation became faster for large systems, further tests must be performed in order to check whether this advantage is kept or even increased in the flexible case.

1. INTRODUCTION

During the last years, several efficient methods for the real-time simulation of rigid multibody systems have been developed. The performance enhancement experienced by computers makes the inclusion of new features possible, like flexibility and contact. But all these new features have a negative effect on efficiency, making the achievement of real-time simulation more difficult, so that new efforts must be carried out regarding the dynamic formulations, in order to perform more realistic, real-time simulations.

Most real-time methods for the dynamics of rigid multibody systems take advantage of the mechanism topology and, therefore, are called topological (they use

relative coordinates). Although more difficult to implement than global methods (those using Cartesian or fully Cartesian coordinates), they have proven to be more efficient for large systems (Cuadrado et al. (2004)).

The purpose of this work is to extend a topological formulation for rigid bodies to the flexible case, and to compare its behavior with that of a global formulation, as it has been previously done for rigid multibody systems.

2. GLOBAL AND TOPOLOGICAL METHODS

Two methods, one global and another topological, are considered in this work. The global method is a floating frame of reference (FFR) formulation (Shabana (1998)) based on natural coordinates, as described in Cuadrado et al. (2001). The new topological method combines the approach used to address flexibility by the global one, with a rigid body topological semi-recursive formulation which has showed excellent results for large rigid multibody systems (Cuadrado et al. (2004)).

The global FFR formulation is based on natural coordinates. Each flexible body has a local frame of reference attached to it, which is defined by a point at the origin and three orthogonal unit vectors along the axes. This frame experiences the large amplitude motion, and deformations are added on local coordinates, by using component mode synthesis to reduce the model size.

In the rigid case, the topological method, semi-recursive, opens the closed loops to get the associated open loop mechanism, and defines such system with relative coordinates. In order to obtain the dynamic equations, an intermediate set of global Cartesian coordinates is defined at body level (three translations plus three rotations), and then a velocity transformation is carried out to project the equations

into the relative coordinates. This projection is recursively performed by accumulation of forces and inertias, taking advantage of the mechanism topology. Then, closed loop conditions must be imposed through the corresponding constraints, implemented in natural global coordinates.

In both methods, the equations of motion, stated through an index-3 augmented Lagrangian formulation, are combined with the integrator (trapezoidal rule), to produce a nonlinear algebraic system of equations with the dependent positions as unknowns (Cuadrado et al. (1997)), solved by Newton-Raphson iteration. Once convergence is attained into the time-step at position level, velocities and accelerations are projected for them to satisfy the first and second derivatives of the constraints.

3. THE PROPOSED FORMULATION

The equations of motion, according to an index-3 augmented Lagrangian formulation in relative dependent coordinates, are stated in the form,

$$\mathbf{M}\ddot{\mathbf{z}} + \Phi_z^T \alpha \Phi + \Phi_z^T \lambda^* = \mathbf{Q} \quad (1)$$

where \mathbf{z} is the relative coordinates vector, \mathbf{M} is the mass matrix, Φ is the closed loop constraints vector, Φ_z is its Jacobian matrix, \mathbf{Q} is the vector of elastic, applied and velocity-dependent forces, and λ^* is the Lagrange multipliers vector, obtained from an iteration process carried out within each time-step,

$$\lambda_{i+1}^* = \lambda_i^* + \alpha \Phi_{i+1} \quad i = 0, 1, 2, \dots \quad (2)$$

which starts with λ_0^* equal to the value of λ^* obtained in the previous time-step.

3.1 Flexible Body Modeling

The position of an arbitrary point \mathbf{r} of a deformed body is defined as follows,

$$\mathbf{r} = \mathbf{r}_0 + \mathbf{A}\bar{\mathbf{r}} = \mathbf{r}_0 + \mathbf{A}(\bar{\mathbf{r}}_u + \bar{\mathbf{q}}_f) \quad (3)$$

where \mathbf{r}_0 stands for the position of the origin of the local frame of reference, \mathbf{A} is a rotation matrix defined by the three orthogonal unit vectors of the reference frame $[\mathbf{u}|\mathbf{v}|\mathbf{w}]$, $\bar{\mathbf{r}}_u$ is the undeformed position of the point in local coordinates, and $\bar{\mathbf{q}}_f$ is its local elastic displacement.

The elastic deformation is obtained by means of a finite element model of the body, which generally contains a large number of degrees of freedom (DOFs), so that a model reduction must be carried out to reduce computation times. In the proposed method, a Craig-Bampton reduction (Craig and Bampton (1968)) is used, since it allows for an easy coupling

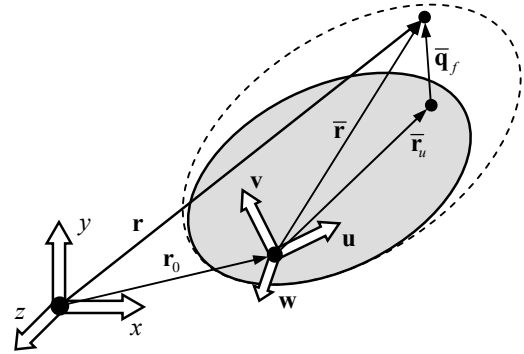


Figure 1 General flexible body.

between bodies, and is particularly well suited for a topological implementation, as will be seen later. This reduction method approximates the elastic displacement field by a linear combination of static and dynamic modes, which can be pre-computed using any finite element code.

Following the natural coordinates formalism, the body is connected to the rest of the mechanism by means of boundary points and unit vectors. Boundary points and vectors are associated to finite element displacement and rotation DOFs respectively, so that each static mode is obtained as the displacement field resulting from applying a unit variation to one of these boundary DOFs while keeping the remaining fixed. Dynamic modes are normal eigenmodes calculated with a fixed interface configuration. All static and dynamic modes are calculated with the body clamped at the local frame of reference.

At this point, the topological implementation shows some particular characteristics. In the global formulation, the frame of reference terms \mathbf{r}_0 and \mathbf{u} , \mathbf{v} , \mathbf{w} , are problem variables, while in the topological one they are calculated when the kinematic problem is recursively solved for the open loop system, at each time-step, to obtain the joint positions. This avoids the need for additional constraints to ensure that the three vectors are orthonormal. Moreover, compatibility constraints are no longer needed to link the static modal amplitudes to the boundary points and unit vectors, since they are directly obtained while solving the kinematics.

Using this reduction, the local elastic displacement that appears in Eq. (3) can be expressed as a linear combination of deformation modes,

$$\bar{\mathbf{q}}_f = \sum_i^{ns} \Phi_i \eta_i + \sum_j^{nd} \Psi_j \xi_j \quad (4)$$

where Φ_i and Ψ_j are the static and dynamic modes, and η_i and ξ_j are their respective modal amplitudes, which are added as new coordinates of the multibody system. This expression

can be written in matrix form,

$$\bar{\mathbf{q}}_f = \begin{bmatrix} \Phi_1 & \dots & \Phi_{ns} & \Psi_1 & \dots & \Psi_{nd} \end{bmatrix} \begin{Bmatrix} \eta_1 \\ \dots \\ \eta_{ns} \\ \xi_1 \\ \dots \\ \xi_{nd} \end{Bmatrix} = \mathbf{X}\mathbf{y} \quad (5)$$

being \mathbf{X} a matrix formed by the modes as columns, and \mathbf{y} a vector containing all the modal amplitudes of the body.

3.2 Positions and velocities

Topological methods cut the closed loops to establish recursive relationships. These loops are then closed by the corresponding kinematic constraints. To calculate the body dynamic terms, an intermediate global Cartesian coordinate vector \mathbf{Z} is defined at velocity level for each body,

$$\mathbf{Z} = \begin{Bmatrix} \dot{\mathbf{s}} \\ \boldsymbol{\omega} \end{Bmatrix} \quad (6)$$

In this vector, $\dot{\mathbf{s}}$ is the velocity of the point of the body which instantly coincides with the origin of the global frame of reference, considering the point as rigidly attached to the body local frame (Bae and Haug (1987)), and $\boldsymbol{\omega}$ is the angular velocity vector of the local frame of reference. These coordinates are related to the rigid body motion, and the global velocity vector for a flexible body, after the addition of the modal amplitudes, is,

$$\dot{\mathbf{q}} = \begin{Bmatrix} \dot{\mathbf{s}} \\ \boldsymbol{\omega} \end{Bmatrix} = \begin{Bmatrix} \mathbf{Z} \\ \dot{\mathbf{y}} \end{Bmatrix} \quad (7)$$

The rigid body velocity vector \mathbf{Z}_i of an element i can be obtained for an open loop mechanism by means of a recursive relationship (Funes et al. (2004)),

$$\mathbf{Z}_i = \mathbf{Z}_{i-1} + \mathbf{b}_i \dot{z}_i + \boldsymbol{\phi}_{i-1,i} \dot{\boldsymbol{\eta}}_{i-1,i} - \boldsymbol{\phi}_{i,i} \dot{\boldsymbol{\eta}}_{i,i} \quad (8)$$

To illustrate this expression, Fig. 2 shows a planar revolute joint between two deformed bodies $i-1$ and i . \mathbf{Z}_{i-1} is the absolute velocity of the preceding body frame in the kinematic chain. The \mathbf{z}_i vector contains all the relative coordinates defined at joint i , so that each \mathbf{b}_i matrix column is the relative velocity that arises when giving a unit velocity to the corresponding relative coordinate. In the example, z_i is the relative angle at the joint. Vectors $\boldsymbol{\eta}_{i-1,i}$ and $\boldsymbol{\eta}_{i,i}$ are the amplitudes of the static modes defined at joint i for bodies $i-1$

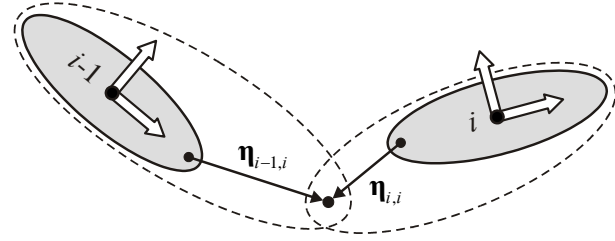


Figure 2 Recursive kinematics in a planar revolute joint.

and i respectively (i.e. the local elastic displacement vectors of the boundary point), so that the $\boldsymbol{\phi}$ terms have an analogous meaning to the \mathbf{b} ones due to how the static modes are defined. The \mathbf{b} and $\boldsymbol{\phi}$ terms depend on the joint and mode type (translational or rotational) respectively, and are functions of the positions. In the particular case of a body whose frame of reference is placed at its entry point, the last term in Eq. (8) doesn't appear, since the body is clamped at its local frame origin.

Accelerations can be calculated by time differentiation of Eq. (8),

$$\dot{\mathbf{Z}}_i = \dot{\mathbf{Z}}_{i-1} + \mathbf{b}_i \ddot{z}_i + \boldsymbol{\phi}_{i-1,i} \ddot{\boldsymbol{\eta}}_{i-1,i} - \boldsymbol{\phi}_{i,i} \ddot{\boldsymbol{\eta}}_{i,i} + \dot{\mathbf{d}}_i + \dot{\boldsymbol{\phi}}_{i-1,i} \dot{\boldsymbol{\eta}}_{i-1,i} - \dot{\boldsymbol{\phi}}_{i,i} \dot{\boldsymbol{\eta}}_{i,i} \quad (9)$$

where \mathbf{d}_i stands for $\dot{\mathbf{b}}_i \dot{z}_i$.

Equations (8) and (9) yield the velocities and accelerations of the local frames of reference. Differentiation of Eq. (3) particularized to a finite element node n yields its velocity \mathbf{v}_n^* as a function of its absolute position \mathbf{r}_n^* and the body coordinates \mathbf{q} ,

$$\mathbf{v}_n^* = \dot{\mathbf{s}} + \boldsymbol{\omega} \times \mathbf{r}_n^* + \mathbf{A}(\mathbf{X}_n^* \dot{\mathbf{y}}) \quad (10)$$

where \mathbf{X}_n^* is the submatrix formed by the three rows of \mathbf{X} corresponding to the elastic displacements of node n . This expression can be written in matrix form to include the velocities of all the mn nodes,

$$\mathbf{v}^* = \begin{Bmatrix} \mathbf{v}_1^* \\ \mathbf{v}_2^* \\ \dots \\ \mathbf{v}_{mn}^* \end{Bmatrix} = \begin{bmatrix} \mathbf{I}_3 & -\tilde{\mathbf{r}}_1^* & \mathbf{A}\mathbf{X}_1^* \\ \mathbf{I}_3 & -\tilde{\mathbf{r}}_2^* & \mathbf{A}\mathbf{X}_2^* \\ \dots & \dots & \dots \\ \mathbf{I}_3 & -\tilde{\mathbf{r}}_{mn}^* & \mathbf{A}\mathbf{X}_{mn}^* \end{bmatrix} \begin{Bmatrix} \dot{\mathbf{s}} \\ \boldsymbol{\omega} \\ \dot{\mathbf{y}} \end{Bmatrix} = \mathbf{B}\dot{\mathbf{q}} \quad (11)$$

where the tilde denotes the skew-symmetric matrix associated to the corresponding vector. The velocities of all the nodes, required for the calculation of the inertia terms, are therefore expressed as a function of the body coordinates \mathbf{q} .

3.3 Dynamic Terms in Cartesian Coordinates

The kinetic energy of a body can be expressed as,

$$T = \frac{1}{2} \int_V \dot{\mathbf{r}}^T \dot{\mathbf{r}} dm \quad (12)$$

where V is the volume of the deformed body. For the calculation of this integral, the co-rotational approximation proposed by Geradin and Cardona (2001) is used. This approximation, which leads to a simplified mass matrix at the cost of introducing a kinematic inconsistency, assumes that the finite element interpolation functions \mathbf{N} , intended for the interpolation of elastic displacements, can be used as well for the interpolation of velocities. In that case, the kinetic energy can be approximated in terms of the finite element mass matrix \mathbf{M}_{FEM} and the nodal velocities \mathbf{v}^* ,

$$T = \frac{1}{2} \int_V \mathbf{v}^{*T} \mathbf{N}^T \mathbf{N} \mathbf{v}^* dm = \frac{1}{2} \mathbf{v}^{*T} \mathbf{M}_{FEM} \mathbf{v}^* \quad (13)$$

These nodal velocities can be calculated by using the \mathbf{B} matrix defined in Eq. (11), so that the mass matrix $\bar{\mathbf{M}}$ of an elastic body in body coordinates is obtained as,

$$T = \frac{1}{2} \dot{\mathbf{q}}^T \mathbf{B}^T \mathbf{M}_{FEM} \mathbf{B} \dot{\mathbf{q}} \Rightarrow \bar{\mathbf{M}} = \mathbf{B}^T \mathbf{M}_{FEM} \mathbf{B} \quad (14)$$

This is a very simple expression for the mass matrix, taking into account that the finite element mass matrix is directly obtained from a standard finite element code and is constant. Application of the Lagrange equations to this expression of the kinetic energy leads to the velocity dependent inertia forces,

$$\bar{\mathbf{Q}}_v = -\mathbf{B}^T \mathbf{M}_{FEM} \dot{\mathbf{B}} \dot{\mathbf{q}} \quad (15)$$

The elastic potential of a deformed body is obtained from the finite element stiffness matrix \mathbf{K}_{FEM} and the nodal elastic displacements,

$$U = \frac{1}{2} \bar{\mathbf{q}}_f^{*T} \mathbf{K}_{FEM} \bar{\mathbf{q}}_f^* \quad (16)$$

The elastic displacements of the nodes from Eq. (5) can be introduced into this equation, so that a stiffness matrix \mathbf{K} is obtained in terms of the modal amplitudes,

$$U = \frac{1}{2} \mathbf{y}^T \mathbf{X}^T \mathbf{K}_{FEM} \mathbf{X} \mathbf{y} \Rightarrow \mathbf{K} = \mathbf{X}^T \mathbf{K}_{FEM} \mathbf{X} \quad (17)$$

and this constant matrix can be used for the calculation of the elastic forces,

$$\bar{\mathbf{Q}}_e = -\frac{\partial U}{\partial \mathbf{q}} = -\mathbf{K} \mathbf{y} \quad (18)$$

Applied forces are introduced in body coordinates by means of the virtual power principle. For example, for a point force \mathbf{F} applied at node \mathbf{r}_i ,

$$\bar{\mathbf{Q}}_a^T \dot{\mathbf{q}} = \mathbf{F}^T \dot{\mathbf{r}}_i \Rightarrow \bar{\mathbf{Q}}_a = \left(\frac{\partial \mathbf{r}_i}{\partial \mathbf{q}} \right)^T \mathbf{F} = \mathbf{B}_i^T \mathbf{F} \quad (19)$$

where \mathbf{B}_i is the three row submatrix of \mathbf{B} corresponding to the three degrees of freedom of node i .

3.4 Equations of Motion

In order to make the following steps clearer, the coordinates of the whole system will be grouped into two vectors, one for each coordinate set,

$$\begin{aligned} \dot{\mathbf{q}} &= \left\{ \mathbf{Z}_1^T \quad \dots \quad \mathbf{Z}_{nb}^T \quad \dot{\boldsymbol{\eta}}_1^T \quad \dots \quad \dot{\boldsymbol{\eta}}_{nb}^T \quad \dot{\boldsymbol{\xi}}_1^T \quad \dots \quad \dot{\boldsymbol{\xi}}_{nb}^T \right\}^T \\ \dot{\mathbf{z}} &= \left\{ \dot{z}_1 \quad \dots \quad \dot{z}_{nc} \quad \dot{\boldsymbol{\eta}}_1^T \quad \dots \quad \dot{\boldsymbol{\eta}}_{nb}^T \quad \dot{\boldsymbol{\xi}}_1^T \quad \dots \quad \dot{\boldsymbol{\xi}}_{nb}^T \right\}^T \end{aligned} \quad (20)$$

where nb stands for the number of bodies in the system, and nc is the number of relative coordinates of the open loop version of the mechanism. The mass matrix and force vector in body coordinates can be assembled for the whole system, having separate blocks for the rigid body part, the static modal amplitudes, and the dynamic modal amplitudes,

$$\bar{\mathbf{M}} = \begin{bmatrix} \bar{\mathbf{M}}_{RB} & \bar{\mathbf{M}}_{RB,\eta} & \bar{\mathbf{M}}_{RB,\xi} \\ \bar{\mathbf{M}}_{\eta,RB} & \bar{\mathbf{M}}_{\eta} & \bar{\mathbf{M}}_{\eta,\xi} \\ \bar{\mathbf{M}}_{\xi,RB} & \bar{\mathbf{M}}_{\xi,\eta} & \bar{\mathbf{M}}_{\xi} \end{bmatrix}; \quad \bar{\mathbf{Q}} = \begin{Bmatrix} \bar{\mathbf{Q}}_{RB} \\ \bar{\mathbf{Q}}_{\eta} \\ \bar{\mathbf{Q}}_{\xi} \end{Bmatrix} \quad (21)$$

The application of the virtual power principle yields,

$$\dot{\mathbf{q}}^{*T} (\bar{\mathbf{M}} \dot{\mathbf{q}} - \bar{\mathbf{Q}}) = 0 \quad (22)$$

equation that must be transformed into the set of relative coordinates \mathbf{z} . They are related to the body coordinates \mathbf{q} by a transformation matrix \mathbf{R} such that,

$$\dot{\mathbf{q}} = \mathbf{R} \dot{\mathbf{z}} \quad (23)$$

Substitution of \mathbf{q} and its derivatives in Eq. (22) results in the following expression for the equations of motion, taking into account that the \mathbf{z} coordinates are independent for an open-loop system,

$$\mathbf{R}^T \bar{\mathbf{M}} \mathbf{R} \dot{\mathbf{z}} = \mathbf{R}^T (\bar{\mathbf{Q}} - \bar{\mathbf{M}} \dot{\mathbf{R}} \dot{\mathbf{z}}) \quad (24)$$

This means that the leading matrix and the right hand side of the equations of motion in relative coordinates are,

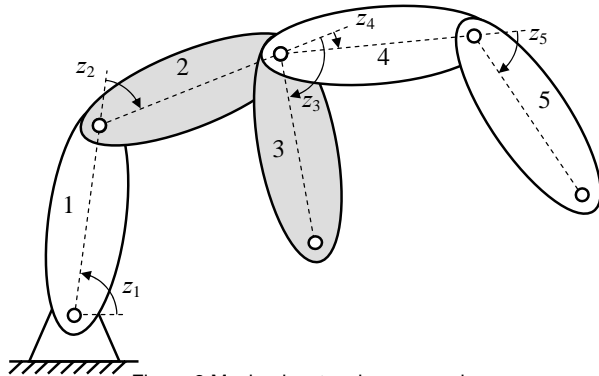


Figure 3 Mechanism topology example.

$$\mathbf{M} = \mathbf{R}^T \bar{\mathbf{M}} \mathbf{R} \quad ; \quad \mathbf{Q} = \mathbf{R}^T (\bar{\mathbf{Q}} - \bar{\mathbf{M}} \dot{\mathbf{R}} \mathbf{z}) \quad (25)$$

These operations can be performed very efficiently by taking advantage of the open loop topology. The \mathbf{R} matrix is the result of assembling in matrix form the recursive relationships defined in Eq. (8) for the open loop system, which makes its structure rather particular. Matrix \mathbf{R} can be divided into blocks if the \mathbf{q} and \mathbf{z} coordinates are arranged as described in Eq. (20),

$$\mathbf{R} = \begin{bmatrix} \mathbf{R}_{RB} & \mathbf{R}_\eta & \mathbf{0} \\ \mathbf{0} & \mathbf{I} & \mathbf{0} \\ \mathbf{0} & \mathbf{0} & \mathbf{I} \end{bmatrix} \quad (26)$$

where \mathbf{R}_{RB} and \mathbf{R}_η are two submatrices which relate the Cartesian coordinates to the relative coordinates and to the static modal amplitudes, respectively. The first submatrix, the rigid body part of \mathbf{R} , would be the \mathbf{R} matrix of an equivalent rigid mechanism in the current deformed configuration. The example described in Fig. 3, in which bodies 2 and 3 are flexible, is used to show how the \mathbf{R} matrix terms look like,

$$\mathbf{R}_{RB} = \begin{bmatrix} \mathbf{I}_6 & \mathbf{0} & \mathbf{0} & \mathbf{0} & \mathbf{0} \\ \mathbf{I}_6 & \mathbf{I}_6 & \mathbf{0} & \mathbf{0} & \mathbf{0} \\ \mathbf{I}_6 & \mathbf{I}_6 & \mathbf{I}_6 & \mathbf{0} & \mathbf{0} \\ \mathbf{I}_6 & \mathbf{I}_6 & \mathbf{0} & \mathbf{I}_6 & \mathbf{0} \\ \mathbf{I}_6 & \mathbf{I}_6 & \mathbf{0} & \mathbf{I}_6 & \mathbf{I}_6 \end{bmatrix} \begin{bmatrix} \mathbf{b}_1 & \mathbf{0} & \mathbf{0} & \mathbf{0} & \mathbf{0} \\ \mathbf{0} & \mathbf{b}_2 & \mathbf{0} & \mathbf{0} & \mathbf{0} \\ \mathbf{0} & \mathbf{0} & \mathbf{b}_3 & \mathbf{0} & \mathbf{0} \\ \mathbf{0} & \mathbf{0} & \mathbf{0} & \mathbf{b}_4 & \mathbf{0} \\ \mathbf{0} & \mathbf{0} & \mathbf{0} & \mathbf{0} & \mathbf{b}_5 \end{bmatrix} = \mathbf{T}_{RB} \mathbf{R}_{RB}^d \quad (27)$$

$$\mathbf{R}_\eta = \begin{bmatrix} \mathbf{0} & \mathbf{0} & \mathbf{0} & \mathbf{0} \\ \mathbf{I}_6 & \mathbf{0} & \mathbf{0} & \mathbf{0} \\ \mathbf{I}_6 & \mathbf{I}_6 & \mathbf{I}_6 & \mathbf{0} \\ \mathbf{I}_6 & \mathbf{I}_6 & \mathbf{0} & \mathbf{0} \\ \mathbf{I}_6 & \mathbf{I}_6 & \mathbf{0} & \mathbf{0} \end{bmatrix} \begin{bmatrix} -\boldsymbol{\varphi}_{2,2} & \mathbf{0} & \mathbf{0} & \mathbf{0} \\ \mathbf{0} & \boldsymbol{\varphi}_{2,34} & \mathbf{0} & \mathbf{0} \\ \mathbf{0} & \mathbf{0} & -\boldsymbol{\varphi}_{3,3} & \mathbf{0} \\ \mathbf{0} & \mathbf{0} & \mathbf{0} & \mathbf{0} \end{bmatrix} = \mathbf{T}_\eta \mathbf{R}_\eta^d$$

Each of these two submatrices can be considered as the

product of a connectivity matrix \mathbf{T} , which depends exclusively on the mechanism topology, and a block diagonal matrix \mathbf{R}^d , containing the kinematic \mathbf{b} or $\boldsymbol{\varphi}$ terms. Each block column of the connectivity matrices is associated to either a joint (RB) or a boundary generating static modes (η), and contains identity matrices in the rows corresponding to those bodies being affected by a variation of the column's relative coordinates or modal amplitudes. Expanding in blocks the mass matrix projection of Eq. (25) (Funes et al. (2004)),

$$\mathbf{R}^T \bar{\mathbf{M}} \mathbf{R} = \begin{bmatrix} \mathbf{R}_{RB}^T \bar{\mathbf{M}}_{RB} \mathbf{R}_{RB} & \mathbf{R}_{RB}^T \bar{\mathbf{M}}_{RB} \mathbf{R}_\eta & \mathbf{0} \\ \mathbf{R}_\eta^T \bar{\mathbf{M}}_{RB} \mathbf{R}_{RB} & \mathbf{R}_\eta^T \bar{\mathbf{M}}_{RB} \mathbf{R}_\eta & \mathbf{0} \\ \mathbf{0} & \mathbf{0} & \mathbf{0} \end{bmatrix} + \begin{bmatrix} \mathbf{0} & \mathbf{0} & \mathbf{0} \\ \mathbf{0} & \bar{\mathbf{M}}_\eta & \bar{\mathbf{M}}_{\eta,\xi} \\ \mathbf{0} & \bar{\mathbf{M}}_{\xi,\eta} & \bar{\mathbf{M}}_\xi \end{bmatrix} \quad (28)$$

$$+ \begin{bmatrix} \mathbf{0} & \mathbf{R}_{RB}^T \bar{\mathbf{M}}_{RB,\eta} & \mathbf{R}_{RB}^T \bar{\mathbf{M}}_{RB,\xi} \\ \bar{\mathbf{M}}_{\eta,RB} \mathbf{R}_{RB} & \mathbf{R}_\eta^T \bar{\mathbf{M}}_{RB,\eta} + \bar{\mathbf{M}}_{\eta,RB} \mathbf{R}_\eta & \mathbf{R}_\eta^T \bar{\mathbf{M}}_{RB,\xi} \\ \bar{\mathbf{M}}_{\xi,RB} \mathbf{R}_{RB} & \bar{\mathbf{M}}_{\xi,RB} \mathbf{R}_\eta & \mathbf{0} \end{bmatrix}$$

The same should be done for the force vector. All of these terms can be recursively calculated by accumulating the individual mass matrices from the leaves to the root. For example, the rigid body part of the mass matrix

$$\mathbf{R}_{RB}^T \bar{\mathbf{M}}_{RB} \mathbf{R}_{RB} = \mathbf{R}_{RB}^{dT} (\mathbf{T}_{RB}^T \bar{\mathbf{M}}_{RB} \mathbf{T}_{RB}) \mathbf{R}_{RB}^d \quad (29)$$

For the mechanism shown in Fig. 3,

$$\mathbf{T}_{RB}^T \bar{\mathbf{M}}_{RB} \mathbf{T}_{RB} = \begin{bmatrix} \mathbf{M}_1 & \mathbf{M}_2 & \mathbf{M}_3 & \mathbf{M}_4 & \mathbf{M}_5 \\ & \mathbf{M}_2 & \mathbf{M}_3 & \mathbf{M}_4 & \mathbf{M}_5 \\ & & \mathbf{M}_3 & \mathbf{0} & \mathbf{0} \\ & & & \mathbf{M}_4 & \mathbf{M}_5 \\ & & & & \mathbf{M}_5 \end{bmatrix} \quad (30)$$

sym

where the \mathbf{M}_i sub-matrices are the following,

$$\begin{aligned} \mathbf{M}_5 &= \bar{\mathbf{M}}_5 \\ \mathbf{M}_4 &= \bar{\mathbf{M}}_4 + \mathbf{M}_5 \\ \mathbf{M}_3 &= \bar{\mathbf{M}}_3 \\ \mathbf{M}_2 &= \bar{\mathbf{M}}_2 + \mathbf{M}_3 + \mathbf{M}_4 \\ \mathbf{M}_1 &= \bar{\mathbf{M}}_1 + \mathbf{M}_2 \end{aligned} \quad (31)$$

All the remaining terms of the mass matrix can be calculated following a similar procedure, taking advantage on

the connectivity matrices, and the same can be said of the projected force vector.

Once the dynamic terms have been obtained in relative coordinates for the open loop system, the closed loop kinematic constraints are imposed in natural coordinates. The Jacobian matrix of the constraints appearing in Eq. (1) is evaluated by differentiating the constraints with respect to the relative coordinates, which can be done by means of the chain differentiation rule,

$$\Phi_z = \Phi_q \mathbf{q}_z \quad (32)$$

where in this case \mathbf{q} stands for the natural coordinates at the corresponding cut joint. The term \mathbf{q}_z is easily calculated since each column contains the velocities of the natural coordinates when a unit velocity is given to its corresponding relative coordinate z and zero to the rest.

3.5 Time Integration

The numerical integrator adopted is the implicit single-step trapezoidal rule, whose difference equations are,

$$\begin{aligned} \dot{\mathbf{z}}_{n+1} &= \frac{2}{\Delta t} \mathbf{z}_{n+1} + \hat{\mathbf{z}}_n \\ \ddot{\mathbf{z}}_{n+1} &= \frac{4}{\Delta t^2} \mathbf{z}_{n+1} + \hat{\ddot{\mathbf{z}}}_n \end{aligned} \quad (33)$$

where Δt is the time-step and,

$$\begin{aligned} \hat{\mathbf{z}}_n &= -\left(\frac{2}{\Delta t} \mathbf{z}_n + \dot{\mathbf{z}}_n \right) \\ \hat{\ddot{\mathbf{z}}}_n &= -\left(\frac{4}{\Delta t^2} \mathbf{z}_n + \frac{4}{\Delta t} \dot{\mathbf{z}}_n + \ddot{\mathbf{z}}_n \right) \end{aligned} \quad (34)$$

If dynamic equilibrium is imposed at step $n+1$ by combining the integrator equations (33) with the equations of motion (1), a nonlinear system of algebraic equations must be solved for the relative coordinates in $n+1$,

$$\mathbf{f}(\mathbf{z}_{n+1}) = 0 \quad (35)$$

The system can be solved using the Newton-Raphson iteration with the following approximated tangent matrix and residual vector,

$$\begin{aligned} \mathbf{f}_z &\cong \mathbf{M} + \frac{\Delta t}{2} \mathbf{C} + \frac{\Delta t^2}{4} (\Phi_z^T \alpha \Phi_z + \mathbf{K}) \\ \mathbf{f} &= \frac{\Delta t^2}{4} (\mathbf{M} \ddot{\mathbf{q}} + \Phi_z^T \alpha \Phi_z + \Phi_z^T \lambda^* - \mathbf{Q}) \end{aligned} \quad (36)$$

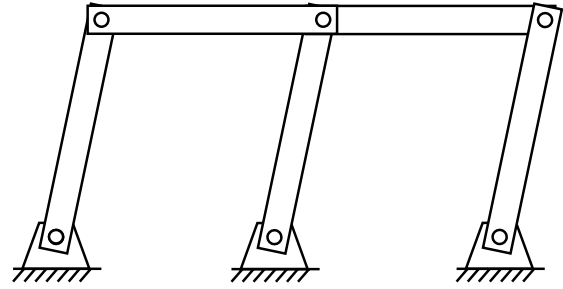


Figure 4 Double four-bar mechanism.

being \mathbf{K} and \mathbf{C} the stiffness and damping matrices,

$$\mathbf{K} = -\mathbf{Q}_z \quad ; \quad \mathbf{C} = -\mathbf{Q}_z \quad (37)$$

The solution of Eq. (35) yields a position vector that fulfills the dynamic equilibrium equations and the kinematic constraints at position level $\Phi = 0$. However, the velocities and accelerations do not satisfy the derivatives of the constraints, since they have not been imposed. Therefore, the resulting velocities and accelerations need to be projected in order to enforce their fulfillment of the constraints derivatives. Naming $\dot{\mathbf{z}}^*$ and $\ddot{\mathbf{z}}^*$ the velocities and accelerations obtained once the Newton-Raphson iteration has converged, the new projected velocities and accelerations are obtained solving the following linear systems,

$$\begin{aligned} \mathbf{f}_z \dot{\mathbf{z}} &= \left[\mathbf{M} + \frac{\Delta t}{2} \mathbf{C} + \frac{\Delta t^2}{4} \mathbf{K} \right] \dot{\mathbf{z}}^* - \frac{\Delta t^2}{4} \Phi_z^T \alpha \Phi_t \\ \mathbf{f}_z \ddot{\mathbf{z}} &= \left[\mathbf{M} + \frac{\Delta t}{2} \mathbf{C} + \frac{\Delta t^2}{4} \mathbf{K} \right] \ddot{\mathbf{z}}^* - \frac{\Delta t^2}{4} \Phi_z^T \alpha (\Phi_z \dot{\mathbf{z}} + \dot{\Phi}_t) \end{aligned} \quad (38)$$

4 TEST EXAMPLES

Two examples, already used for a global vs topological comparison in rigid multibody systems, have been implemented in Matlab environment through both the global and the topological formulation. The first one is a planar double four-bar mechanism, formed by five identical bars, and the second one is the front left suspension of the Iltis vehicle. Performance measurements have been carried out with different numbers of flexible elements, in order to evaluate the influence of such parameter in each formulation.

4.1. Double Four-Bar Mechanism

The system consists of five identical steel bars, each of them having unit length and mass, connected by revolute joints. Each bar can be considered as rigid or flexible, modeled in the flexible case by 10 beam elements, with one

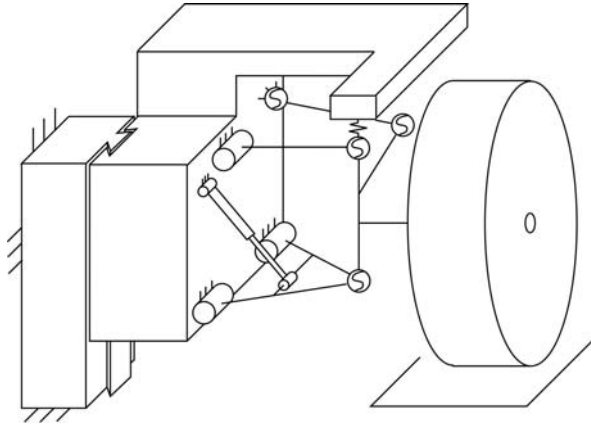


Figure 5 Iltis suspension.

axial static, one bending static, and two bending dynamic modes. The number of coordinates varies as more flexible bars are considered in the system, being this variation different in the global and topological formulations, because the latter doesn't include as coordinates the unit vectors of the local frames. The number of coordinates for each formulation and number of flexible bodies is given in Table 1.

Table 1 Number of system coordinates in the first example.

# flexible bars	0	1	2	3	4	5
Global	6	13	20	27	34	41
Topological	5	8	11	14	17	20

The number of coordinates tends to be double in the global case when more flexible bodies are considered, because each flexible body adds four modal amplitudes plus four unit vector components, while, in the topological case, each body adds only the four modal amplitudes.

The system is subject to gravity acceleration, and is given an initial velocity of 1 rad/s in clockwise direction. Motion is integrated during 5 s, the time to approximately complete 2.7 revolutions. The time-step used in all simulations is 10 ms, and the CPU-times required for the integration are those provided in Table 2.

Table 2 CPU-times (s) in the first example.

# flex.	0	1	2	3	4	5
Global	0,91	3,30	6,24	9,61	11,51	15,22
Topolog.	4,85	9,11	12,62	15,74	17,74	20,92

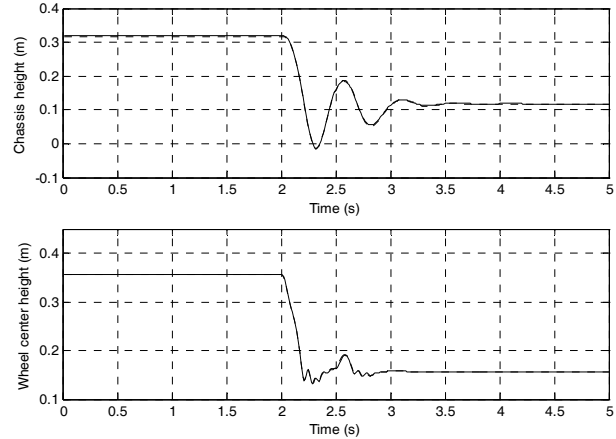


Figure 6 Iltis suspension simulation results.

As it may be seen in the table, the CPU-times reduce their difference when more bodies are considered flexible. In the rigid case, the global formulation is five times faster, while, in the fully flexible model, the topological formulation needs only 37% more time for integration, probably due to the proportionally lower number of coordinates mainly.

4.2. Iltis Suspension

The front left suspension of the Bombardier Iltis vehicle (Iltis Data Package (1990)) consists, as shown in Fig. 5, on a lower A-arm triangle connected to both the car body and the wheel hub. A damper connects the A-arm to the car body, and the upper side of the hub is connected to the chassis by means of a leaf spring, which is modeled as an articulated bar with a spring element added between the hub top and the chassis. In this system, three elements can be considered as flexible: the A-arm, the bar that models the leaf spring, and the steering rod. All of them have been modeled as steel elements, with 10 elements per bar (two bending static modes and four bending dynamic modes) and 21 elements in the case of the A-arm (one vertical static mode in the connection to the hub, another one in the connection to the damper, and the first two dynamic modes). The number of coordinates of all the possible combinations of formulation and number of flexible bodies results,

Table 3 Number of system coordinates in the second example.

# flexible elements	0	1	2	3
Global	25	38	53	68
Topological	8	12	18	24

In this case, the number of coordinates of the global model is around three times larger, and, unlike the previous example, this relation remains almost constant with the number of flexible bodies.

The suspension reaches equilibrium and then runs down a 0.2 m step at $t=2$ s. The integration, with a time-step of 10 ms, is carried out for 5 seconds until the suspension reaches equilibrium again. The time history of the vertical coordinate of the chassis as well as that of the wheel center are plotted in Fig. 6, showing a very good agreement between the two formulations (dotted line for the topological method). The CPU-times required to carry out the simulation are displayed in Table 4.

Table 4 CPU-times (s) in the second example.

# flex.	0	1	2	3
Global	1,95	9,05	14,56	19,43
Topolog.	8,19	20,54	29,55	38,57

In this three-dimensional case, the performance difference is reduced when more flexible bodies are considered, as it happened in the planar case. The CPU-time ratio changes from a value of 4 in the rigid case, to a value of 2 when the three mentioned bodies are modeled as flexible.

CONCLUSIONS

A new topological formulation for flexible multibody dynamics has been presented, and its performance compared with that of a global formulation. The new formulation obtains lower performance than the global one in the two cases studied, but some considerations should be taken into account:

1. The simulated systems were not large enough to extract definitive conclusions. In the rigid case, the topological formulation was slower in both examples, but results were totally different for larger systems (Cuadrado et al. (2004)). Moreover, the topological method tends to improve its relative performance as more bodies are modeled as flexible.

2. The formulations were implemented in Matlab, where matrix multiplications are calculated by compiled internal functions and, hence, are very fast, while m-code is very inefficient. This motivated that calculation of the mass matrix and force vector of Eq. (25) by means of the accumulation method described in section 3.4, is slower than by direct multiplication. Consequently, direct multiplication was used in the examples, thus losing the theoretical advantage provided by the recursive accumulation of masses and forces. Different results would be obtained if the examples were

implemented in C++ or Fortran languages.

3. The **B** matrix calculation and mass matrix projection take between 30% and 60% of the total integration time. The impact of these operations obviously grows with the number of flexible bodies, being higher in the global case. Either a further reduction procedure, or a preprocess for obtaining constant mass matrix terms instead of keeping the size of the underlying finite element model -as it happens with the **B** matrix- would also affect the results.

Therefore, further work must be carried out in order to determine the efficiency of the topological formulation and to establish application criteria of the global and the topological formulations in the flexible case, as it was done for systems of rigid bodies. The simulation of a large system -like the full model of the Iltis vehicle-, implemented in either C++ or Fortran languages, will likely provide the information needed to achieve the final conclusions.

REFERENCES

- Bae, D.S. and Haug, E.J., A Recursive Formulation for Constrained Mechanical System Dynamics. Part I - Open Loop Systems, *Mechanics of Structures and Machines*, Vol. 5, No. 2, pp. 359-382, 1987.
- Craig, R.R. and Bampton, M.C.C., Coupling of Substructures for Dynamic Analyses, *AIAA Journal*, Vol. 6, No. 7, pp. 1313-1319, 1968.
- Cuadrado, J., Cardenal, J. and Bayo, E., Modeling and Solution Methods for Efficient Real-Time Simulation of Multibody Dynamics, *Multibody System Dynamics*, Vol. 1, No. 3, pp. 259-280, 1997.
- Cuadrado, J., Gutierrez, R., Naya, M.A. and Morer, P., A Comparison in Terms of Accuracy and Efficiency Between a MBS Dynamic Formulation with Stress Analysis and a Non-Linear FEA Code, *International Journal for Numerical Methods in Engineering*, Vol. 51, No. 9, pp. 1033-1052, 2001.
- Cuadrado, J., Dopico, D., Gonzalez, M. and Naya, M.A., A Combined Penalty and Recursive Real-Time Formulation for Multibody Dynamics, *Journal of Mechanical Design*, Vol. 126, No. 4, pp. 602-608, 2004.
- Funes, F.J., Garcia de Jalon, J., de Ribera, F.A. and Alvarez, E., Resolucion de la Dinamica de Sistemas Flexibles Mediante Formulaciones Topologicas, *Proceedings of Metodos Computacionais em Engenharia*, Lisbon, 2004.
- Geradin, M. and Cardona, A., *Flexible Multibody Dynamics - A Finite Element Approach*, John Wiley and Sons, New York, 2001.
- Iltis Data Package, *IATSD Workshop*, Herbertov, 1990.
- Shabana, A.A., *Dynamics of Multibody Systems*, 2nd edition, Cambridge University Press, Cambridge, 1998.